

Central exclusive production of scalar and pseudoscalar charmonia in the light-front k_T -factorization approach

Izabela Babiarz,^{1,*} Roman Pasechnik,^{2,†} Wolfgang Schäfer,^{1,‡} and Antoni Szczurek^{1,3,§}

¹*Institute of Nuclear Physics, Polish Academy of Sciences,
ul. Radzikowskiego 152, PL-31-342 Kraków, Poland*

²*Department of Astronomy and Theoretical Physics,
Lund University, SE-223 62 Lund, Sweden*

³*Faculty of Mathematics and Natural Sciences,
University of Rzeszów, ul. Pigońia 1, PL-35-310 Rzeszów, Poland*

Abstract

We study exclusive production of scalar $\chi_{c0} \equiv \chi_c(0^{++})$ and pseudoscalar η_c charmonia states in proton-proton collisions at the LHC energies. The amplitudes for $gg \rightarrow \chi_{c0}$ as well as for $gg \rightarrow \eta_c$ mechanisms are derived in the k_T -factorization approach. The $pp \rightarrow pp\eta_c$ reaction is discussed for the first time. We have calculated rapidity, transverse momentum distributions as well as such correlation observables as the distribution in relative azimuthal angle and (t_1, t_2) distributions. The latter two observables are very different for χ_{c0} and η_c cases. In contrast to the inclusive production of these mesons considered very recently in the literature, in the exclusive case the cross section for η_c is much lower than that for χ_{c0} which is due to a special interplay of the corresponding vertices and off-diagonal UGDFs used to calculate the cross sections. We present the numerical results for the key observables in the framework of potential models for the light-front quarkonia wave functions. We also discuss how different are the absorptive corrections for both considered cases.

PACS numbers: 12.38.Bx, 13.85.Ni, 14.40.Pq

* izabela.babiarz@ifj.edu.pl

† roman.pasechnik@thep.lu.se

‡ Wolfgang.Schafer@ifj.edu.pl

§ antoni.szczurek@ifj.edu.pl

I. INTRODUCTION

The central exclusive diffractive processes in proton-proton collisions at high energies have attracted recently a lot of attention. These processes lead to very unusual final states. For example, in the central exclusive production one produces one or a few particles at central rapidities which are fully measured. There are no other tracks in the detectors. The incoming protons remain intact (in the virtue of “elastic diffraction”) or are excited into small mass hadronic systems, which disappear into the beam pipe. We consider here simultaneously two such reactions, $pp \rightarrow p \chi_{c0} p$ and $pp \rightarrow p \eta_c p$, which are well suited to be analysed in the framework of the so-called Durham model formulated by Khoze, Martin and Ryskin (see Ref. [1] and references therein). From the experimental point of view, there is a rapidity gap, between each of the protons and the produced χ_{c0} or η_c states. These processes hence provide a very clean environment for the study of the produced hadronic systems tightly connected to poorly known soft and semi-hard QCD dynamics. For a review of conceptual and experimental challenges with such central exclusive production (CEP) reactions, see for example Ref. [2].

The theory of the CEP of single χ_{cJ} , $J = 0, 1, 2$ mesons, with a correct account for the spin of the mesons and precise kinematics of the production process has been worked out earlier by Pasechnik, Szczurek and Teryaev (PST) in a series of papers [3–5]. The numerical calculations were done for the Tevatron energies. In this analysis, the non-relativistic QCD (NRQCD) methods were applied. So far, only CEP of light pseudoscalar mesons was discussed in the literature [3, 6]. There rather nonperturbative effects strongly dominate (see Ref. [6]). Very recently in Ref. [7] the production of χ_{c0} at the LHC was discussed in the k_T -factorisation and saturation dipole-model inspired approaches. The analysis was performed there in the NRQCD approach and using a single model for the unintegrated gluon distribution (UGDs) and a particular prescription for the off-diagonal UGD. Given a particular importance of the CEP of heavy quarkonia for ongoing and future experimental studies, we revisit and extend this analysis to account for additional effects and sources for theoretical uncertainties (such as the shapes of the charmonia wave functions and a treatment of the absorptive corrections, as well as an accurate treatment of the phase space and production kinematics) as well as incorporate the pseudoscalar η_c final state for the first time.

Recently our group showed how to include relativistic corrections for the inclusive production of η_c [8] and very recently for inclusive production of χ_{c0} [9] using the light-cone wave functions of the charmonia derived from the well-known $c\bar{c}$ interquark potential models. It is the aim of the present paper to do a similar study for the exclusive case. In addition, there

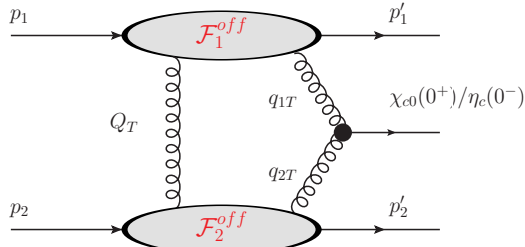


FIG. 1. Generic diagram for the Durham model approach to the considered exclusive production processes.

is no such a study on the $pp \rightarrow pp\eta_c$ CEP available in the literature. In contrast, $\eta_c(1S)$ was measured by the LHCb collaboration in the inclusive case for $\sqrt{s} = 7, 8, 13$ TeV [10]. Is such a measurement possible for the exclusive production of η_c ? This study is a first step to address this important question. An analysis of inclusive diffractive production of $\eta_c(1S)$ was done recently in [11].

In the present paper, we wish to discuss in parallel the exclusive production process of both the scalar χ_{c0} and pseudoscalar η_c quarkonia. For illustration of the corresponding production mechanism initially proposed by the Durham group [1], see Fig. 1. We start with a brief introduction into the formalism for $pp \rightarrow p\chi_{c0}p$ and $pp \rightarrow p\eta_cp$ reactions based upon the Durham model of CEP [1] setting up the necessary notation and conventions. In this model, a quarkonium state is produced via fusion of two virtual active gluons accompanied by an extra exchange with a screening gluon as is shown in Fig. 1. The additional exchange of the gluon provides colour conservation and hence the effective color singlet exchange in the t -channel. As a result, in the final state, in addition to the meson produced mainly at central rapidities, there are two forward protons that retain most of their initial energy. We intend to calculate the integrated cross sections for such processes as well as several differential distributions relevant for future measurements. We wish to discuss both the hard and soft processes involved in these reactions in the light-front QCD approach, to consider several prescriptions on how to calculate the off-diagonal UGDs (some of them have already been used previously in the literature) and to estimate the absorptive corrections in the differential distributions.

II. VIRTUAL GLUON FUSION INTO PSEUDO(SCALAR) CHARMONIA

Below, we shall consider the hard $\chi_{c0}(1P)$ and $\eta_c(1S)$ charmonia production subprocesses separately.

A. The light-cone amplitude for $g^*g^* \rightarrow \chi_{c0}(1P)$ process

The gluon-gluon fusion vertex is proportional to the reduced amplitude $\mathcal{T}_{\mu\nu}$ as follows:

$$\mathcal{V}_{\mu\nu}^{ab}(g^*g^* \rightarrow \chi_{c0}) = 4\pi\alpha_s \frac{\text{Tr}[t^a t^b]}{\sqrt{N_c}} 2\mathcal{T}_{\mu\nu} = \frac{4\pi\alpha_s}{\sqrt{N_c}} \delta^{ab}\mathcal{T}_{\mu\nu}, \quad (2.1)$$

$$\mathcal{T}_{\mu\nu} = -\delta_{\mu\nu}^\perp(q_1, q_2)G_{\text{TT}}(q_1^2, q_2^2) + e_\mu^L(q_1)e_\nu^L(q_2)G_{\text{LL}}(q_1^2, q_2^2), \quad (2.2)$$

where α_s is the strong coupling, $N_c = 3$ and t^a are the number of colors and $SU(3)$ group generators in QCD, respectively, and

$$\begin{pmatrix} G_{\text{TT}} \\ G_{\text{LL}} \end{pmatrix} = \begin{pmatrix} -|\mathbf{q}_1||\mathbf{q}_2| & (q_1 \cdot q_2) \\ (q_1 \cdot q_2) & -|\mathbf{q}_1||\mathbf{q}_2| \end{pmatrix} \begin{pmatrix} G_1 \\ G_2 \end{pmatrix}, \quad (2.3)$$

while the relevant kinematical variables are displayed in Fig. 1. Here, we have the projector on transverse polarization states

$$-\delta_{\mu\nu}^\perp(q_1, q_2) = -g_{\mu\nu} + \frac{1}{X} \left((q_1 \cdot q_2)(q_{1\mu}q_{2\nu} + q_{1\nu}q_{2\mu}) - q_1^2 q_{2\mu}q_{2\nu} - q_2^2 q_{1\mu}q_{1\nu} \right), \quad (2.4)$$

with $X = (q_1 \cdot q_2)^2 - q_1^2 q_2^2$. The longitudinal polarization vectors read as follows

$$e_\mu^L(q_1) = \sqrt{\frac{-q_1^2}{X}} \left(q_{2\mu} - \frac{q_1 \cdot q_2}{q_1^2} q_{1\mu} \right), \quad e_\nu^L(q_2) = \sqrt{\frac{-q_2^2}{X}} \left(q_{1\nu} - \frac{q_1 \cdot q_2}{q_2^2} q_{2\nu} \right). \quad (2.5)$$

The convoluted form of reduced amplitude can be written as

$$\mathcal{T} = n_\nu^+ n_\mu^- \mathcal{T}_{\mu\nu} = |\mathbf{q}_1| |\mathbf{q}_2| G_1(q_1^2, q_2^2) + (\mathbf{q}_1 \cdot \mathbf{q}_2) G_2(q_1^2, q_2^2), \quad (2.6)$$

in terms of the light cone vectors $n_\nu^\pm = (1, 0, 0, \pm 1)$. The form factors here $G_i(\mathbf{q}_1^2, \mathbf{q}_2^2)$ have the integral representations in terms of the P -wave charmonia wave function $\psi_\chi(z, \mathbf{k})$ (see Ref. [9] for more details)

$$\begin{aligned} G_1(\mathbf{q}_1^2, \mathbf{q}_2^2) &= |\mathbf{q}_1| |\mathbf{q}_2| \frac{4m_c}{\mathbf{q}_2^2} \int \frac{dz d^2 \mathbf{k}}{z(1-z)16\pi^3} \psi_\chi(z, \mathbf{k}) 2z(1-z)(2z-1) \left[\frac{1}{\mathbf{l}_A^2 + \varepsilon^2} - \frac{1}{\mathbf{l}_B^2 + \varepsilon^2} \right] \\ G_2(\mathbf{q}_1^2, \mathbf{q}_2^2) &= 4m_c \int \frac{dz d^2 \mathbf{k}}{z(1-z)16\pi^3} \psi_\chi(z, \mathbf{k}) \left[\frac{1-z}{\mathbf{l}_A^2 + \varepsilon^2} + \frac{z}{\mathbf{l}_B^2 + \varepsilon^2} \right] \\ &\quad + \frac{4m_c}{\mathbf{q}_2^2} \int \frac{dz d^2 \mathbf{k}}{z(1-z)16\pi^3} \psi_\chi(z, \mathbf{k}) 4z(1-z) \left[\frac{\mathbf{q}_2 \cdot \mathbf{l}_A}{\mathbf{l}_A^2 + \varepsilon^2} - \frac{\mathbf{q}_2 \cdot \mathbf{l}_B}{\mathbf{l}_B^2 + \varepsilon^2} \right], \end{aligned} \quad (2.7)$$

where z is a c -quark (or \bar{c} -antiquark) momentum fraction, \mathbf{k} is the relative $c\bar{c}$ transverse momentum, m_c is the mass of c -quark, and the shorthand notations

$$\varepsilon^2 = z(1-z)\mathbf{q}_1^2 + m_c^2, \quad \mathbf{l}_A = \mathbf{k} - (1-z)\mathbf{q}_2, \quad \mathbf{l}_B = \mathbf{k} + z\mathbf{q}_2, \quad (2.8)$$

have been introduced.

B. The light cone amplitude for $g^* g^* \rightarrow \eta_c$ process

In Ref. [8], we introduced the covariant form of the vertex for two off-shell gluon fusion into η_c meson:

$$\mathcal{V}_{\mu\nu}^{ab} = (-i)4\pi\alpha_s \epsilon_{\mu\nu\alpha\beta} q^\alpha q^\beta \frac{\delta^{ab}}{2\sqrt{N_c}} 2I(\mathbf{q}_1^2, \mathbf{q}_2^2), \quad (2.9)$$

where $I(\mathbf{q}_1^2, \mathbf{q}_2^2) = F_{\gamma^* \gamma^* \rightarrow \eta_c}(\mathbf{q}_1^2, \mathbf{q}_2^2)/(e_c^2 \sqrt{N_c})$. The convoluted form reads:

$$\mathcal{V}^{ab}(g^* g^* \rightarrow \eta_c) = (-i)4\pi\alpha_s \frac{\delta^{ab}}{\sqrt{N_c}} \mathbf{q}_1 \times \mathbf{q}_2 I(\mathbf{q}_1^2, \mathbf{q}_2^2), \quad (2.10)$$

$$\mathcal{V}^{ab} = (-i)4\pi\alpha_s \frac{\delta^{ab}}{\sqrt{N_c}} I(\mathbf{q}_1^2, \mathbf{q}_2^2) |\mathbf{q}_1| |\mathbf{q}_2| \sin(\phi_1 - \phi_2), \quad (2.11)$$

and $(\phi_1 - \phi_2)$ is azimuthal angle between \mathbf{q}_1 and \mathbf{q}_2 . We then express $I(\mathbf{q}_1^2, \mathbf{q}_2^2)$ in terms of light-cone wave functions as follows [12]

$$\begin{aligned} I(\mathbf{q}_1^2, \mathbf{q}_2^2) &= 4m_c \int \frac{dz d^2 \mathbf{k}}{z(1-z)16\pi^3} \psi_\eta(z, \mathbf{k}) \left\{ \frac{1-z}{(\mathbf{k} - (1-z)\mathbf{q}_2)^2 + z(1-z)\mathbf{q}_1^2 + m_c^2} \right. \\ &\quad \left. + \frac{z}{(\mathbf{k} + z\mathbf{q}_2)^2 + z(1-z)\mathbf{q}_1^2 + m_c^2} \right\}, \end{aligned} \quad (2.12)$$

where $\psi_\eta(z, \mathbf{k})$ is the wave function of $\eta_c(1S)$ meson.

III. MATRIX ELEMENT FOR $pp \rightarrow ppM$ REACTION

The amplitude for the CEP process for a given meson $V \equiv \chi_{c0}, \eta_c$ reads¹:

$$\mathcal{M} = \frac{s}{2} \pi^2 \frac{1}{2} \frac{\delta_{c_1 c_2}}{N_c^2 - 1} \int d^2 \mathbf{Q} \mathcal{V}^{c_1 c_2} \frac{\mathcal{F}_g^{\text{off}}(x_1, x', \mathbf{Q}^2, \mathbf{q}_1^2, \mu^2, t_1) \mathcal{F}_g^{\text{off}}(x_2, x', \mathbf{Q}^2, \mathbf{q}_2^2, \mu^2, t_2)}{\mathbf{Q}^2 \mathbf{q}_1^2 \mathbf{q}_2^2}, \quad (3.1)$$

in terms of the ‘‘active’’ (fusing into V) $x_{1,2}$ and ‘‘screening’’ x' (connecting both proton lines) gluon momentum fractions. The screening gluon carries a transverse momentum \mathbf{Q} , while the transverse momenta of active gluons are denoted by $\mathbf{q}_1, \mathbf{q}_2$. The generalized unintegrated gluon distributions (UGDs) also depend on the hard scale of the process μ (see below). The $2 \rightarrow 3$ total cross section can be calculated generically as follows:

$$\begin{aligned} \sigma &= \frac{1}{2s} \int |\mathcal{M}|^2 (2\pi)^4 \delta^4(p_1 + p_2 - p'_1 - p'_2 - p_V) \\ &\times \left(\frac{1}{2(2\pi)^3} \right)^3 (dy'_1 d^2 \mathbf{p}'_1) (dy'_2 d^2 \mathbf{p}'_2) (dy d^2 \mathbf{p}_V), \end{aligned} \quad (3.2)$$

or, following a simplification done in Ref. [13], as

$$\sigma = \frac{1}{2s} \frac{1}{2^8 \pi^4 s} \int |\mathcal{M}|^2 dt_1 dt_2 dy d\phi. \quad (3.3)$$

Above, $t_1 = (p_1 - p'_1)^2$, $t_2 = (p_2 - p'_2)^2$ and $\phi \in (0, 2\pi)$ is the relative azimuthal angle between the outgoing protons, s is the pp center-of-mass energy squared, y is rapidity of the outgoing meson V .

IV. DIFFERENT APPROACHES TO OFF-DIAGONAL GLUON DENSITIES

In the forward limit of small $t_{1,2} \rightarrow 0$ corresponding to $\mathbf{Q}^2 \simeq \mathbf{q}_{1,2}^2 \equiv Q_{\perp}^2$, the generalized UGDs in Eq. (3.1) are simplified and are considered as functions of only one transverse momentum, i.e.

$$\mathcal{F}_g^{\text{off}}(x_1, x', \mathbf{Q}^2, \mathbf{q}_1^2, \mu^2, t_1) \rightarrow \mathcal{F}_g^{\text{off}}(x_1, x', Q_{\perp}^2, \mu^2, t_1). \quad (4.1)$$

The Khoze-Martin-Ryskin (KMR) prescription for the off-diagonal (‘‘skewed’’) UGD includes a Sudakov form factor $T_g(q_{\perp}^2, \mu^2)$ and is typically written as [1]

$$\mathcal{F}_{g,\text{KMR}}^{\text{off}}(x, x', Q_{\perp}^2, \mu^2; t) = R_g \frac{d}{d \ln q_{\perp}^2} \left[xg(x, q_{\perp}^2) \sqrt{T_g(q_{\perp}^2, \mu^2)} \right]_{q_{\perp}^2 = Q_{\perp}^2} F(t), \quad (4.2)$$

with gluon virtualities $q_{\perp}^2 \equiv \mathbf{q}^2$ etc playing a role of the momentum scale squared in the collinear gluon density $xg(x, q_{\perp}^2)$, and with the nucleon form factor $F(t)$ often parameterised in the following two ways

$$F(t) = \frac{4m_p^2 - 2.79t}{(4m_p^2 - t)(1 - t/0.71)^2} \quad \text{or} \quad F(t) = \exp\left(\frac{bt}{2}\right), \quad b = 4 \text{ GeV}^{-2}, \quad (4.3)$$

¹ Notice a factor 1/2 in the normalization, due to the fact that we use light-cone vectors fulfilling $n^+ \cdot n^- = 2$, matching the conventions of PST.

with m_p being the proton mass, corresponding to the isoscalar nucleon form factor [14] or the QCD elastic profile factor, respectively. The Sudakov form factor is taken as:

$$T_g(q_\perp^2, \mu^2) = \exp \left[- \int_{q_\perp^2}^{\mu^2} \frac{d\mathbf{k}_\perp^2}{\mathbf{k}_\perp^2} \frac{\alpha_s(k_\perp^2)}{2\pi} \int_0^{1-\Delta} \left[z P_{gg}(z) + \sum_q P_{qg}(z) \right] dz \right], \quad (4.4)$$

with the hard scale $\mu^2 = M_V^2$ and $\Delta = k_\perp/(k_\perp + M_V)$.

Regarding the longitudinal momentum fractions, central diffractive production is dominated by the region $x' \ll x_{1,2} \ll 1$. We thus compute the skewedness correction R_g in Eq. (4.2) using a method proposed and derived for the collinear off-diagonal gluon distributions [15]:

$$R_g = \frac{2^{2\lambda+3} \Gamma(\lambda + 5/2)}{\sqrt{\pi} \Gamma(\lambda + 4)}, \quad \lambda = \frac{d}{d \ln(1/x)} \left[\ln \left(xg(x, q_\perp^2) \right) \right]. \quad (4.5)$$

In a slightly off-forward case $t_{1,2} \neq 0$, the choice of Q_\perp in the off-diagonal KMR gluon in Eq. (4.2) becomes somewhat arbitrary. In practical calculations, we use the so-called ‘‘minimum prescription’’ proposed by the Durham group, by substituting $Q_\perp^2 \rightarrow \min(Q_\perp^2, q_\perp^2)$ in Eq. (4.2), with transverse momentum of an active gluon q_\perp and transverse momentum of the screening gluon Q_\perp . In addition, we suggest a geometrical average of active and screening gluon momenta as $Q_\perp^2 \rightarrow \sqrt{Q_\perp^2 q_\perp^2}$ – an option, called BPSS in the following, for brevity.

We vary our results by also using the modified off-diagonal CDHI gluon defined as [16]

$$\mathcal{F}_{g,\text{CDHI}}^{\text{off}}(x, x', Q_\perp, \mu^2; t) = R_g \left[\frac{\partial}{\partial \log \bar{Q}^2} \sqrt{T_g(\bar{Q}^2, \mu^2)} xg(x, \bar{Q}^2) \right] \cdot \frac{2Q_\perp^2 q_\perp^2}{Q_\perp^4 + q_\perp^4} \cdot F(t), \quad (4.6)$$

where $\bar{Q}^2 = (Q_\perp^2 + q_\perp^2)/2$. In order to take into account the saturation effects, we use of the simplest saturation-based UGD inspired by the Golec-Biernat-Wüsthoff (GBW) model [17]. In order to extrapolate it into the off-diagonal domain, we use the prescription proposed in Ref. [3] (further referred to as the PST prescription):

$$\mathcal{F}_{g,\text{GBW}}^{\text{off}} = \sqrt{f_g^{\text{GBW}}(x', Q_\perp^2) f_g^{\text{GBW}}(x, q_\perp^2)} F(t), \quad f_g^{\text{GBW}}(x, q_\perp^2) = \frac{3\sigma_0}{4\pi^2\alpha_s} R_0^2 q_\perp^2 \exp[R_0^2 q_\perp^2], \quad (4.7)$$

where f_g^{GBW} is the diagonal GBW UGD, and $x' = |\mathbf{Q}|/\sqrt{s}$, $R_0 = \left(\frac{x}{x_0}\right)^\lambda$. In practical calculations, we have used the following fitted values of the GBW parameters: $\sigma_0 = 29.12$ mb, $\lambda = 0.277$, $x_0/10^{-4} = 0.41$, with fixed $\alpha_s = 0.2$.

V. NUMERICAL RESULTS

In the CEP processes at high energies, it is mandatory to consider gluons carrying very small longitudinal momentum fractions x . For this purpose, in practical calculations we use a few parton distribution functions (PDFs) introduced by the Dortmund group: JR14NLO [18] ($Q_{0T}^2 = 0.8 \text{ GeV}^2$), GJR08NLO [19] ($Q_{0T}^2 = 0.5 \text{ GeV}^2$) and GRV94NLO [20] ($Q_{0T}^2 = 0.4 \text{ GeV}^2$). In Fig. 2, we illustrate the shape of the corresponding gluon PDFs at scales and longitudinal momenta typical for the considered $pp \rightarrow pp\eta_c$ and $pp \rightarrow pp\chi_{c,0}$ CEP processes. In the range of scales under discussion, the gluon PDFs from the literature differ

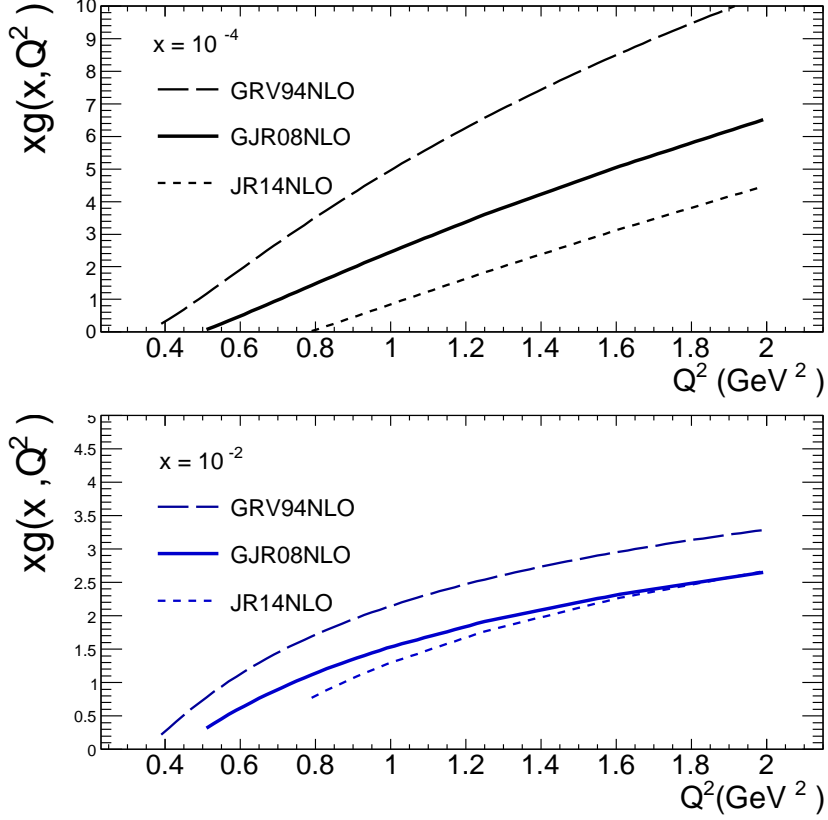


FIG. 2. Collinear gluon PDF as a function of the hard scale of the process and for typical longitudinal gluon momentum fractions, $x = 10^{-4}$ (upper plot) and $x = 10^{-2}$ (lower plot).

considerably. We do not employ the Durham or CTEQ PDFs for which the initial scales for evolution are rather high making them difficult to be applied in the context of the exclusive reactions discussed here.

The total cross sections computed over the full phase space for each PDF mentioned above are listed in Tables 1 and 2, for χ_{c0} and η_c , respectively. The integrated cross section for $pp \rightarrow pp\chi_{c0}$ at $\sqrt{s} = 13$ TeV is shown in Table 1 for different off-diagonal UGD prescriptions for the effective Q_{iT}^2 summarized as follows:

- (a) Durham prescription (Eq. (4.2)): $Q_{iT}^2 = \min(Q_T^2, q_{iT}^2)$,
- (b) BPSS prescription (Eq. (4.2)): $Q_{iT}^2 = \sqrt{Q_T^2 q_{iT}^2}$,
- (c) CDHI prescription (Eq. (4.6)): $Q_{iT}^2 = (Q_T^2 + q_{iT}^2)/2$,
- (d) PST off-diagonal UGD (Eq. (4.7)) .

These prescriptions lead to similar cross sections of the order of $1 \mu\text{b}$ before including absorption effects. The corresponding gap survival factor is of the order of 0.1 as will be discussed at the end of this section.

In Table 2 we present similar results for η_c production. The total cross section for the η_c production is 3-4 orders of magnitude smaller than that for χ_{c0} , i.e. surprisingly small. The cross section for the PST prescription for off-diagonal gluon is quite similar as for the

TABLE 1. Total cross section for χ_{c0} at $\sqrt{s} = 13$ TeV with $R_g = 1.0$ and R_g according to Eq. (4.5). In order to obtain the cross section, several gluon distributions were used with $Q_{0T}^2 \geq 0.4$ GeV² for GRV94NLO, $Q_{0T}^2 \geq 0.5$ GeV² for GJR08NLO, and $Q_{0T}^2 \geq 0.8$ GeV² for JR14NLO. The light-cone form factor for the $gg \rightarrow \chi_{c0}$ coupling was calculated using the Buchmüller-Tye potential (for more details, see Ref. [9]) No gap survival factor is included here.

KMR Skewed gluon $0.8 \text{ GeV}^2 \leq Q_{0T}^2$, JR14NLO	σ_{tot} [nb], $R_g = 1.0$	σ_{tot} [nb], $R_g(x, Q_{iT}^2)$
CDHI, $Q_{iT}^2 = (Q_T^2 + q_{iT}^2)/2$.	$0.65 \cdot 10^3$	$1.50 \cdot 10^3$
KMR, $Q_{iT}^2 = \sqrt{Q_T^2 \cdot q_{iT}^2}$	$0.52 \cdot 10^3$	$1.39 \cdot 10^3$
KMR, $Q_{iT}^2 = \min(Q_T^2, q_{iT}^2)$	$0.27 \cdot 10^3$	$0.52 \cdot 10^3$
KMR Skewed gluon $0.5 \text{ GeV}^2 \leq Q_{0T}^2$, GJR08NLO	σ_{tot} [nb], $R_g = 1.0$	σ_{tot} [nb], $R_g(x, Q_{iT}^2)$
CDHI, $Q_{iT}^2 = (Q_T^2 + q_{iT}^2)/2$.	$0.16 \cdot 10^3$	$0.55 \cdot 10^3$
KMR, $Q_{iT}^2 = \sqrt{Q_T^2 \cdot q_{iT}^2}$	$0.21 \cdot 10^3$	$0.65 \cdot 10^3$
KMR, $Q_{iT}^2 = \min(Q_T^2, q_{iT}^2)$	$0.12 \cdot 10^3$	$0.39 \cdot 10^3$
KMR Skewed gluon $0.4 \text{ GeV}^2 \leq Q_{0T}^2$, GRV94NLO	σ_{tot} [nb], $R_g = 1.0$	σ_{tot} [nb], $R_g(x, Q_{iT}^2)$
CDHI, $Q_{iT}^2 = (Q_T^2 + q_{iT}^2)/2$.	$1.88 \cdot 10^3$	$9.02 \cdot 10^3$
KMR, $Q_{iT}^2 = \sqrt{Q_T^2 \cdot q_{iT}^2}$	$3.03 \cdot 10^3$	$13.4 \cdot 10^3$
KMR, $Q_{iT}^2 = \min(Q_T^2, q_{iT}^2), 0.4 \text{ GeV}^2 \leq Q_{0T}^2$	$1.4 \cdot 10^3$	$6.1 \cdot 10^3$
KMR, $Q_{iT}^2 = \min(Q_T^2, q_{iT}^2), 0.8 \text{ GeV}^2 \leq Q_{0T}^2$	$0.75 \cdot 10^3$	$3.9 \cdot 10^3$
PST Skewed gluon, GBW	σ_{tot} [nb]	-
PST prescription	$2.1 \cdot 10^3$	-

Durham and CDHI prescriptions in the case of χ_{c0} , while the spread in the total cross section for η_c is much higher.

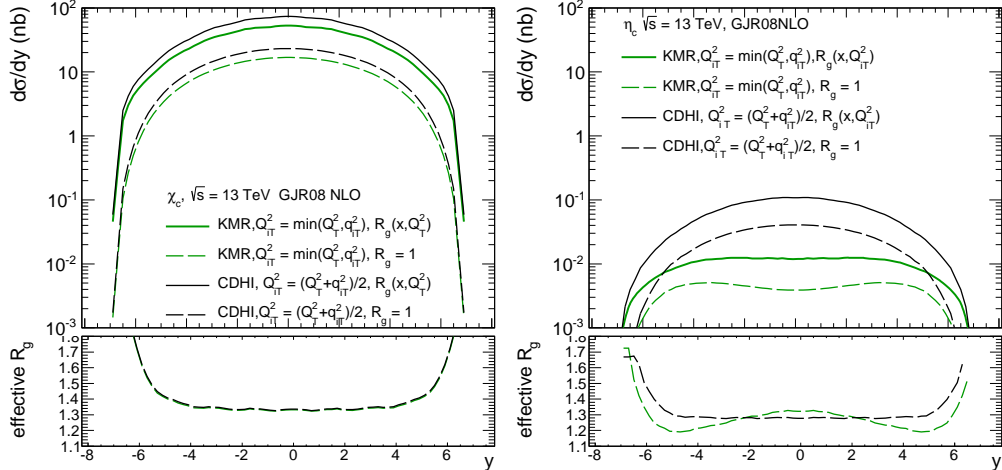


FIG. 3. The rapidity distribution for χ_{c0} , η_c quarkonia CEP and effective R_g factor calculated with the GJR08NLO parton distribution function. No gap survival factor is included here.

In Fig. 3 we show rapidity distribution of $\chi_{c,0}$ (left) and η_c (right) quarkonia CEP. We show results for the Durham (min) and CDHI prescription for the off-diagonal UGDFs. We present results for $R_g = 1$ as well as with R_g calculated according to the Shuvaev prescription

TABLE 2. The same as in Table 1 but for η_c meson. The light-cone form factor for the $gg \rightarrow \eta_c(1S)$ coupling was calculated using the power-law potential (for more details, see Ref. [8])

KMR Skewed gluon, $0.8\text{GeV}^2 \leq Q_{0T}^2$, JR14NLO	σ_{tot} [nb], $R_g = 1.0$	σ_{tot} [nb], $R_g(x, Q_{iT}^2)$
CDHI, $Q_{iT}^2 = (Q_T^2 + q_{iT}^2)/2$.	$1.5 \cdot 10^{-1}$	$3.4 \cdot 10^{-1}$
KMR, $Q_{iT}^2 = \sqrt{Q_T^2 \cdot q_{iT}^2}$	$0.68 \cdot 10^{-1}$	$2.7 \cdot 10^{-1}$
KMR, $Q_{iT}^2 = \min(Q_T^2, q_{iT}^2)$	$0.33 \cdot 10^{-1}$	$0.17 \cdot 10^{-1}$
KMR Skewed gluon, $0.5\text{GeV}^2 \leq Q_{0T}^2$, GJR08NLO	σ_{tot} [nb], $R_g = 1.0$	σ_{tot} [nb], $R_g(x, Q_{iT}^2)$
CDHI, $Q_{iT}^2 = (Q_T^2 + q_{iT}^2)/2$.	$2.9 \cdot 10^{-1}$	$8.1 \cdot 10^{-1}$
KMR, $Q_{iT}^2 = \sqrt{Q_T^2 \cdot q_{iT}^2}$	$1.2 \cdot 10^{-1}$	$4.1 \cdot 10^{-1}$
KMR, $Q_{iT}^2 = \min(Q_T^2, q_{iT}^2), 0.5\text{GeV}^2 \leq Q_{0T}^2$	$0.52 \cdot 10^{-1}$	$1.3 \cdot 10^{-1}$
KMR, $Q_{iT}^2 = \min(Q_T^2, q_{iT}^2), 0.8\text{GeV}^2 \leq Q_{0T}^2$	$0.37 \cdot 10^{-1}$	$0.52 \cdot 10^{-1}$
KMR Skewed gluon, $0.4\text{GeV}^2 \leq Q_{0T}^2$, GRV94NLO	σ_{tot} [nb], $R_g = 1.0$	σ_{tot} [nb], $R_g(x, Q_{iT}^2)$
CDHI, $Q_{iT}^2 = (Q_T^2 + q_{iT}^2)/2$.	$0.37 \cdot 10^4$	$0.76 \cdot 10^4$
KMR, $Q_{iT}^2 = \sqrt{Q_T^2 \cdot q_{iT}^2}$	$0.73 \cdot 10^2$	$1.3 \cdot 10^2$
KMR, $Q_{iT}^2 = \min(Q_T^2, q_{iT}^2), 0.4\text{GeV}^2 \leq Q_{0T}^2$	13	$1.3 \cdot 10^4$
KMR, $Q_{iT}^2 = \min(Q_T^2, q_{iT}^2), 0.8\text{GeV}^2 \leq Q_{0T}^2$	5.8	15.8
PST Skewed gluon, GBW	σ_{tot} [nb]	-
PST prescription	$0.63 \cdot 10^3$	-

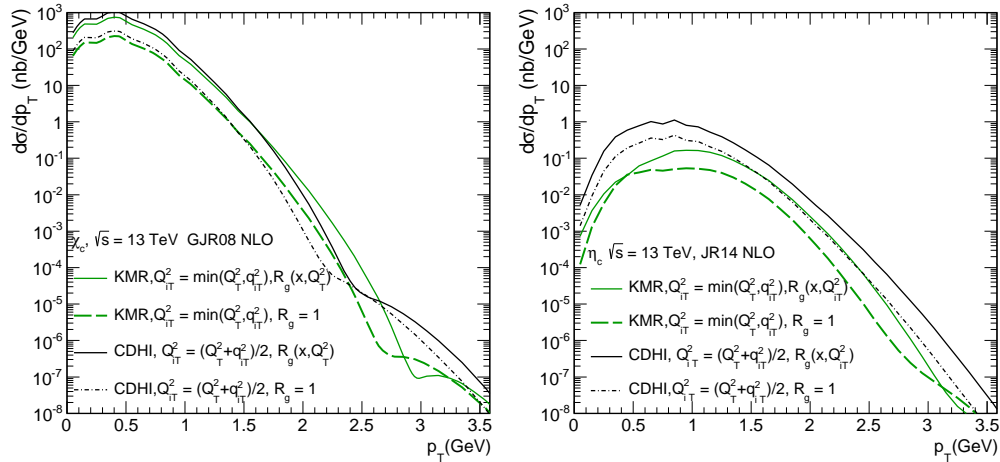


FIG. 4. Distribution in transverse momentum of the χ_{c0} and η_c quarkonia CEP, respectively, with different treatment of R_g factor. No gap survival factor is included here.

(see Eq. (4.5)). Inclusion of R_g increases the cross section by a factor of 3-4. While for χ_{c0} the difference of the results for the Durham prescription and the CDHI prescription is small, for η_c the difference is of the order of magnitude size.

The distribution in transverse momentum are shown in Fig. 4. The distribution for η_c and χ_{c0} CEP are somewhat different. The maximum of the cross-section for η_c is at $p_T \sim 1$ GeV and the dip at vanishing p_T is more pronounced.

In Fig. 5 we show two-dimensional distributions in (t_1, t_2) (t_1, t_2 are four-momenta squared transferred in the proton lines), for $pp \rightarrow pp\eta_c(1S)$. In the left panel we show the result

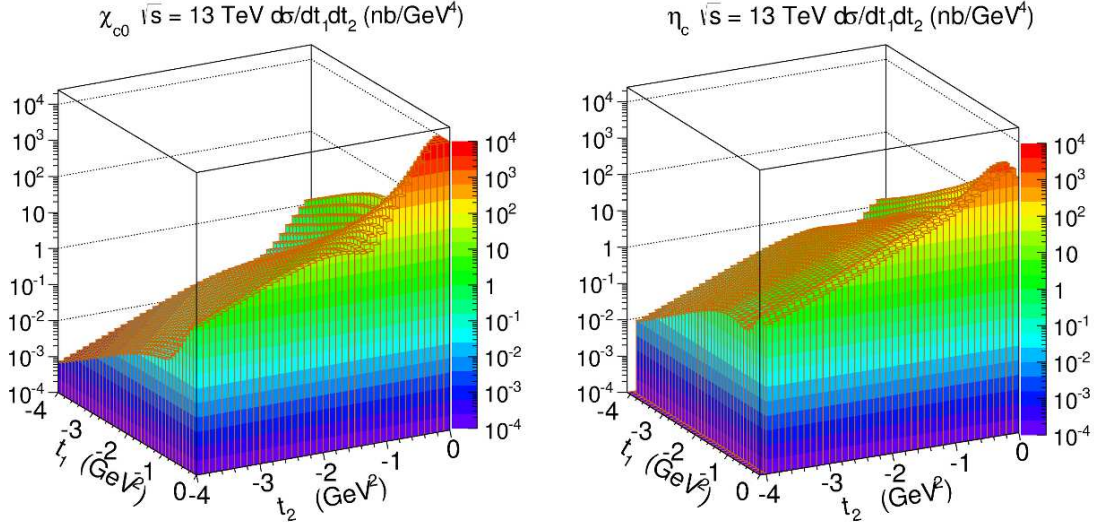


FIG. 5. Differential cross section in $t_1 \times t_2$ at $\sqrt{s} = 13$ TeV for χ_c (left) and η_c (right) CEP processes for the PST off-diagonal UGD computed with the diagonal GBW UGD. No gap survival factor is included here.

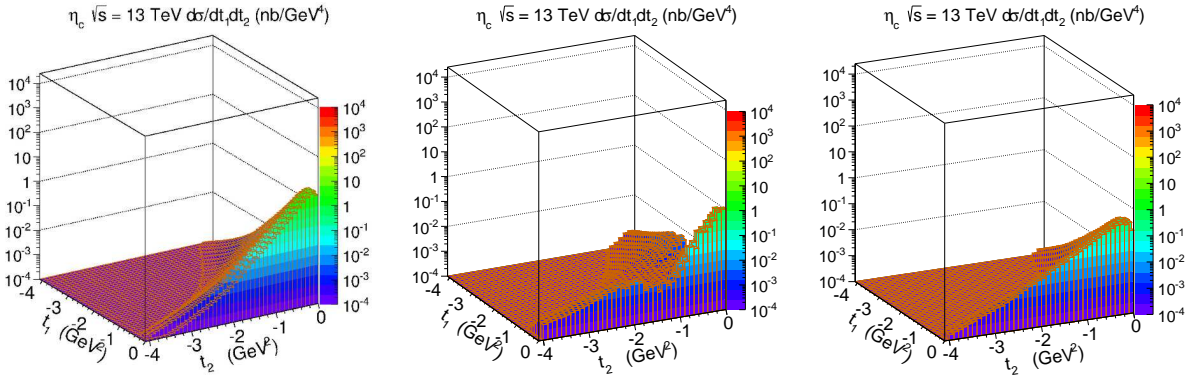


FIG. 6. Distribution in $t_1 \times t_2$ for CDHI (left), BPSS (middle) and Durham (right) prescriptions for η_c CEP for $\sqrt{s} = 13$ TeV calculated with the GJR08NLO gluon distribution function. No gap survival factor is included here.

for the $Q_{it}^2 = \sqrt{q_{it}^2 Q_t^2}$ prescription proposed above for effective transverse momenta used in the KMR method as well as the PST prescription for off-diagonal UGD using the diagonal GBW UGDF. The off-diagonal KMR UGD with the newly proposed prescription leads to some numerical irregularities in the (t_1, t_2) space and extremely small cross sections. In contrast, the distribution for the PST prescription with the GBW UGDF is regular and the corresponding cross section is much larger (see also Table 2).

In Fig. 6 we show similar results for two other prescriptions for the off-diagonal KMR UGDFs: with the Durham prescription – left panel, and the CDHI prescription – right panel. The two prescriptions do not lead to numerical issues but generate extremely small cross sections.

For completeness in Fig. 7 we show similar results for the χ_{c0} production. In contrast to the η_c CEP process, in this case both prescriptions for effective transverse momenta (Durham

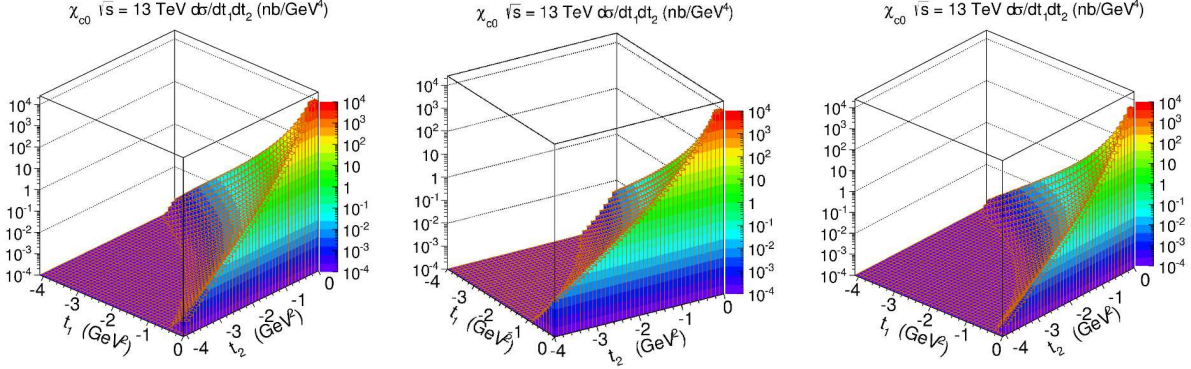


FIG. 7. Distribution in $t_1 \times t_2$ for CDHI (left), BPSS ($Q_{iT}^2 = \sqrt{q_{iT}^2, Q_T^2}$) (middle) and Durham ($Q_{iT}^2 = \min(q_{iT}^2, Q_T^2)$) (right) prescriptions for χ_{c0} for $\sqrt{s} = 13$ TeV calculated with the GJR08NLO gluon distribution function. No gap survival factor is included here.

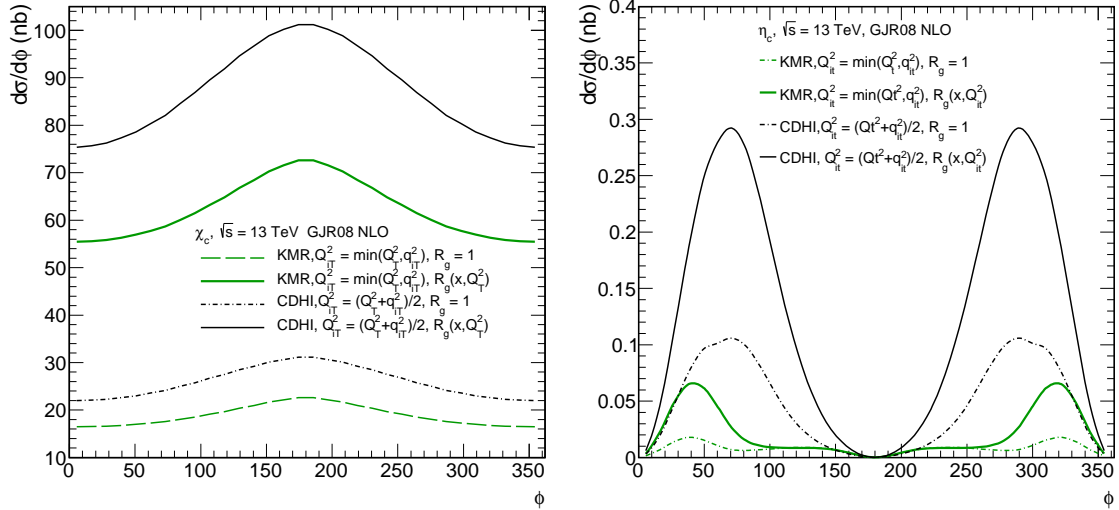


FIG. 8. Distribution in relative azimuthal angle between outgoing protons, for χ_{c0} CEP – left panel, and for η_c CEP – right panel. No gap survival factor is included here.

and CDHI prescriptions) lead to fairly similar results. Here the cross sections are peaked at $t_1 = 0, t_2 = 0$.

In Fig. 8 we show relative azimuthal angle (between outgoing protons) distributions. The distribution for χ_{c0} (left) is very different than that for η_c (right). While for χ_{c0} there is one maximum for the back-to-back configurations, there are two maxima for η_c . The cross section vanishes in the back-to-back kinematics in the case of η_c CEP. The exact position of the maxima depends on the details of the treatment of the off-diagonal UGDs so their experimental identification could pin down the correct theoretical modelling of these objects.

Finally, we wish to compare our results for the exclusive reactions $pp \rightarrow pp\eta_c$ and $pp \rightarrow pp\chi_{c0}$ with their inclusive production counterparts as calculated recently in Refs. [8] and [9]. In Figs. 9 and 10 we show the numerical results (rapidity and transverse momentum distributions) for η_c and χ_{c0} , respectively. While for η_c production the cross section for the

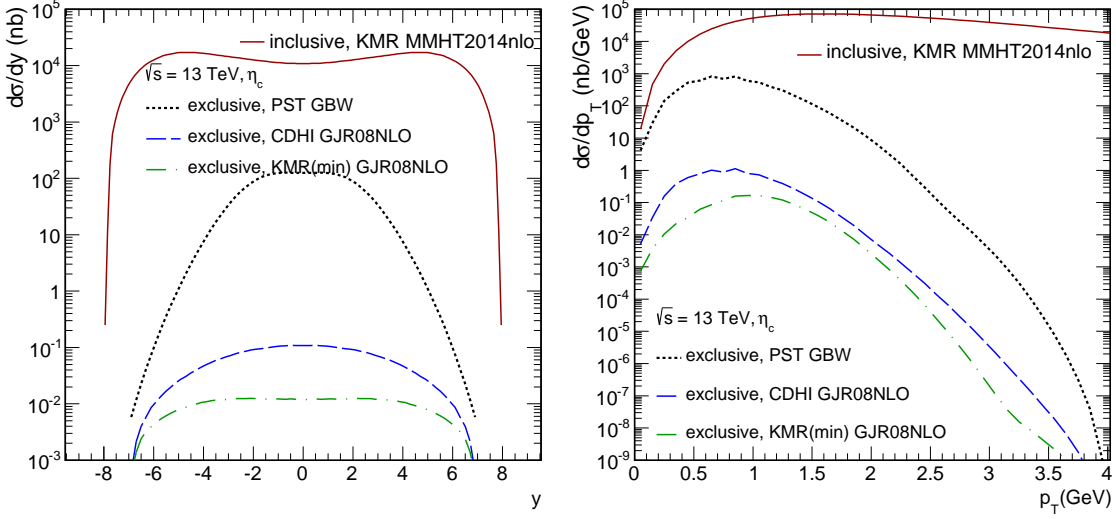


FIG. 9. Comparison of exclusive and inclusive η_c production at $\sqrt{s} = 13$ TeV. No gap survival factor is included for the exclusive reaction.

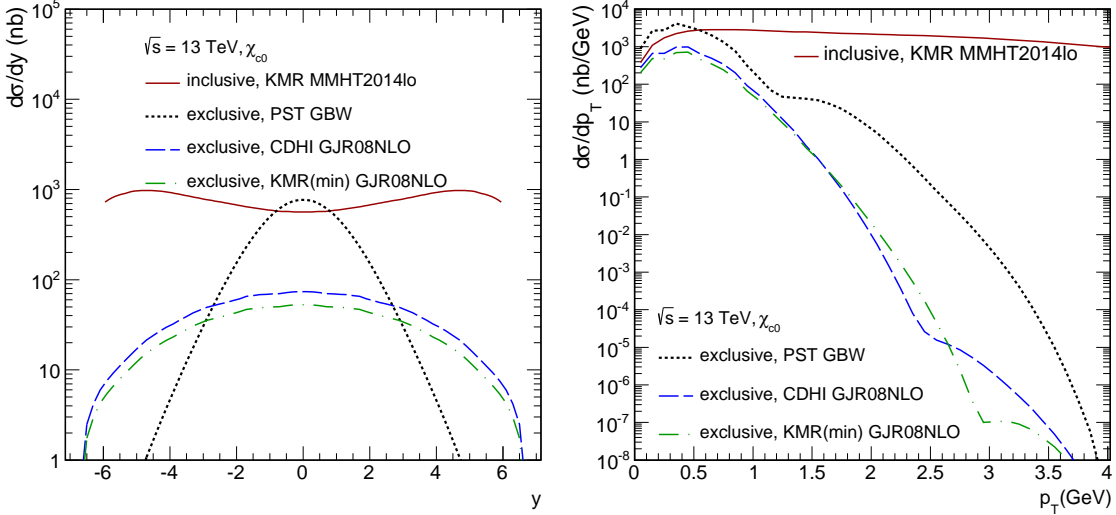


FIG. 10. Comparison of exclusive and inclusive χ_{c0} production at $\sqrt{s} = 13$ TeV. No gap survival factor is included for the exclusive reaction.

exclusive process is a few orders of magnitude lower than that for the inclusive case, this is quite different for χ_{c0} meson. Both for rapidity and transverse momentum distributions the results for the exclusive case are very different compared to the inclusive case.

VI. ABSORPTIVE CORRECTIONS

It is understood that the Born-level cross sections receive absorptive corrections through hadronic rescatterings at large distances. These are related to the interactions of spectator partons [21]. They give rise to the so-called gap survival probability in exclusive reactions. The calculation of the latter poses a difficult problem, which has not been solved yet in a

way fully consistent with the perturbative QCD approach to the production amplitude.

Numerous approaches exist in the literature, some of them are based on soft multi-Pomeron exchanges [22–24], while other approaches avoid the decomposition into Born term and absorptive correction altogether treating the absorptive effects dynamically [25, 26] and at the amplitude level in the dipole picture [27–29], and some of them relate the gap survival probability to the absence of multiparton interactions [30, 31].

It is also understood that the gap survival must depend on the kinematics of the process. Here, we wish to discuss the absorptive corrections at the amplitude level, in a simple quantum-mechanical treatment. To this end, we adopt a simple effective Reggeon Field Theory motivated approach.

In the simplified case where only “elastic rescattering” is taken into account, the amplitude looks as follows:

$$\mathcal{M}(Y, y, \mathbf{p}_1, \mathbf{p}_2) = \mathcal{M}^{(0)}(Y, y, \mathbf{p}_1, \mathbf{p}_2) - \delta\mathcal{M}(Y, y, \mathbf{p}_1, \mathbf{p}_2). \quad (6.1)$$

Here $Y = \log(s/m_p^2)$ is the rapidity difference between the colliding beams at center-of-mass energy \sqrt{s} , y is the cm-rapidity of the produced meson V , and $\mathbf{p}_{1,2}$ are the transverse momenta of outgoing protons.

The absorptive correction is then computed as follows

$$\delta\mathcal{M}(Y, y, \mathbf{p}_1, \mathbf{p}_2) = \int \frac{d^2\mathbf{k}}{2(2\pi)^2} T(s, \mathbf{k}) \mathcal{M}^{(0)}(Y, y, \mathbf{p}_1 + \mathbf{k}, \mathbf{p}_2 - \mathbf{k}), \quad (6.2)$$

with

$$T(s, \mathbf{k}) = \sigma_{\text{tot}}^{pp}(s) \exp\left(-\frac{1}{2}B_{\text{el}}(s)\mathbf{k}^2\right). \quad (6.3)$$

At $\sqrt{s} = 13$ TeV we take $\sigma_{\text{tot}}^{pp} = (110.6 \pm 3.4)$ mb and the nuclear slope $B_{\text{el}} = (20.36 \pm 0.19)$ GeV⁻² [32]. In a double-Regge approach, the Born-level amplitude has the form

$$\mathcal{M}^{(0)}(Y, y, \mathbf{p}_1, \mathbf{p}_2) = is\Phi_1(\mathbf{p}_1)R_{\mathbf{IP}}(Y - y, \mathbf{p}_1^2)V(\mathbf{p}_1, \mathbf{p}_2)R_{\mathbf{IP}}(y, \mathbf{p}_2^2)\Phi_2(\mathbf{p}_2). \quad (6.4)$$

Here, $R_{\mathbf{IP}}(y, \mathbf{p}^2)$ are the Pomeron Regge-propagators, and $V(\mathbf{p}_1, \mathbf{p}_2)$ is the $\mathbf{IPIP} \rightarrow$ Meson vertex.

Let us now briefly discuss the vertices $V(\mathbf{p}_1, \mathbf{p}_2)$. The most general form of the Pomeron-Pomeron-particle vertex for a spinless particle can be written as a Fourier expansion:

$$V(\mathbf{p}_1, \mathbf{p}_2) = V_0(\mathbf{p}_1^2, \mathbf{p}_2^2) + \sum_{n \geq 1} \left(V_n^+(\mathbf{p}_1^2, \mathbf{p}_2^2) \cos(n\phi) + V_n^-(\mathbf{p}_1^2, \mathbf{p}_2^2) \sin(n\phi) \right). \quad (6.5)$$

For a scalar particle, all $V_n^- = 0$, while for the pseudoscalar $V_0 = 0$, $V_n^+ = 0$. For definiteness, let us concentrate on only the first order, $n = 1$. We thus adopt (V^{0+} for scalar and V^{0-} for pseudoscalar state):

$$\begin{aligned} V^{0+}(\mathbf{p}_1, \mathbf{p}_2) &= V_0 + V_1^+(\mathbf{p}_1 \cdot \mathbf{p}_2) = V_0 \left(1 + \tau B_D(\mathbf{p}_1 \cdot \mathbf{p}_2) \right) \quad \text{with} \quad \tau \equiv \frac{V_1^+}{B_D V_0} \\ V^{0-}(\mathbf{p}_1, \mathbf{p}_2) &= V_1^-[\mathbf{p}_1, \mathbf{p}_2]. \end{aligned} \quad (6.6)$$

We further neglect a possible dependence of vertices V_i^\pm on \mathbf{p}_1^2 and \mathbf{p}_2^2 .

TABLE 3. V_0 and V_1 at midrapidity of χ_{c0} , for several prescriptions for off-diagonal UGDs.

χ_{c0}	$V_0^+ [\sqrt{\text{nb}}/\text{GeV}^2]$	τ	$B_D [\text{GeV}^{-2}]$	g_{abs}	β	$\sigma_{\text{tot}} _{y=0} [\text{nb}]$	$\sigma_{\text{tot}}^{\text{abs}} _{y=0} [\text{nb}]$	S^2
PST GBW	-5084	-0.75	5.2	0.73	0.17	154	46	0.30
PST GBW	-5971	-0.70	6.0	0.70	0.19	154	49	0.32
CDHI GJR08NLO	-1856	-0.33	5.5	0.72	0.17	15.12	3.2	0.21
CDHI GJR08NLO	-2550	-0.15	7.4	0.64	0.21	15.12	3.3	0.22
KMR GJR08NLO	-1451	-0.65	5.5	0.72	0.175	10.58	3.18	0.30
KMR GJR08NLO	-2138	-0.11	7.4	0.64	0.210	10.58	2.18	0.20

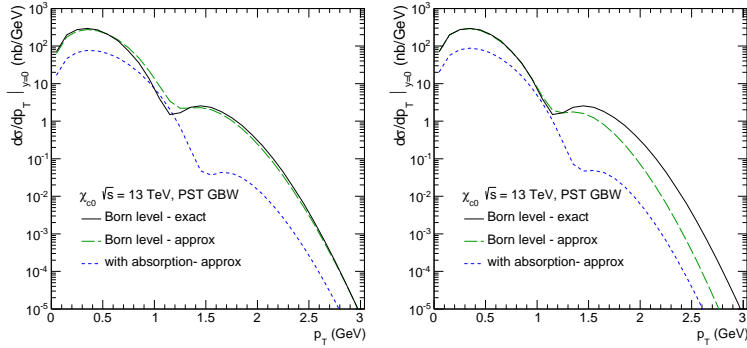


FIG. 11. Transverse momentum distribution of χ_{c0} CEP at $y = 0$, with the PST-GBW prescription with different sets of parameters. On the left hand side, the results are shown with $B_D = 5.2 \text{ GeV}^{-2}$, and on the right hand side – with $B_D = 6.0 \text{ GeV}^{-2}$.

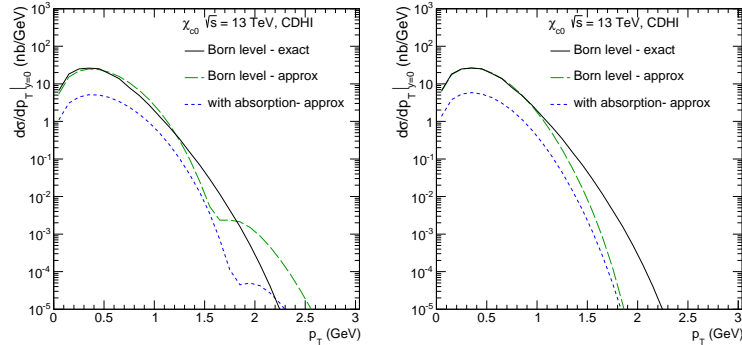


FIG. 12. Distribution in transverse momentum of χ_{c0} CEP with the CDHI prescription with different set of parameters at rapidity $y = 0$. On the left panel, the results are shown with $B_D = 5.5 \text{ GeV}^{-2}$, on the right panel – with $B_D = 7.4 \text{ GeV}^{-2}$.

TABLE 4. An example of V_1 values at midrapidity of η_c in the CEP process, for several prescriptions for off-diagonal UGDs.

η_c	$V_1^- [\sqrt{\text{nb}}/\text{GeV}^4]$	$B_D [\text{GeV}^{-2}]$	g_{abs}	β	$\sigma_{\text{tot}} _{y=0} [\text{nb}]$	$\sigma_{\text{tot}}^{\text{abs}} _{y=0} [\text{nb}]$	S^2
PST GBW	31803.	5.0	0.74	0.16	25	7.0	0.30
CDHI GJR08NLO	834.4	4.6	0.76	0.15	24×10^{-3}	6.9×10^{-3}	0.28
KMR GJR08NLO	285.0	4.2	0.78	0.15	41×10^{-4}	11×10^{-4}	0.26

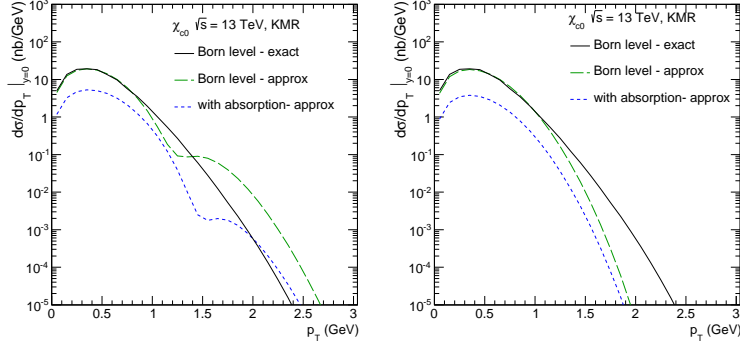


FIG. 13. Distribution in transverse momentum of χ_{c0} with the Durham prescription with different sets of parameters at rapidity $y = 0$. On the left panel, the results are shown with $B_D = 5.5 \text{ GeV}^{-2}$ and on the right panel – with $B_D = 7.4 \text{ GeV}^{-2}$.

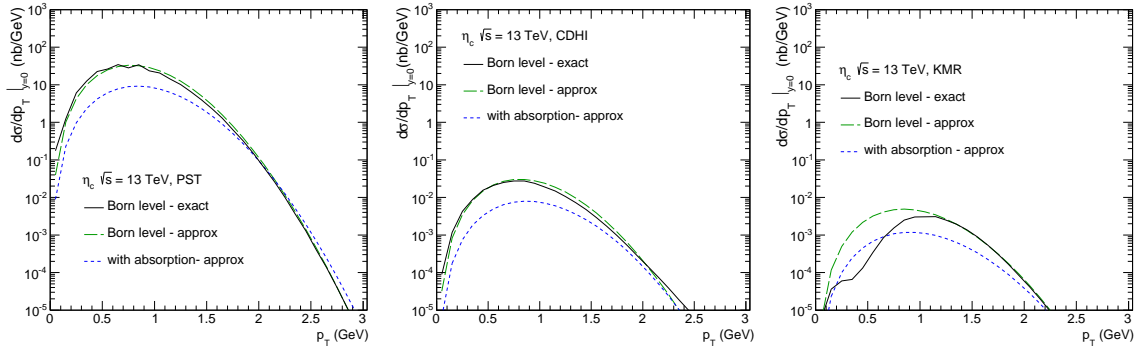


FIG. 14. Distribution in transverse momentum of η_c in the CEP process for PST-GBW, CDHI and Durham prescriptions at $y = 0$.

Our amplitude is normalized in such a way that the expression

$$d\sigma = \frac{1}{512\pi^4 s^2} |\mathcal{M}(Y, y, \mathbf{p}_1, \mathbf{p}_2)|^2 dy d^2\mathbf{p}_1 d^2\mathbf{p}_2 d^2\mathbf{p} \delta^{(2)}(\mathbf{p} + \mathbf{p}_1 + \mathbf{p}_2) \quad (6.7)$$

holds. We will now concentrate on central diffractive production, i.e. we fix the meson rapidity to be $y = 0$. Below we adopt $\sqrt{s} = 13 \text{ TeV}$. We can therefore forget about the Regge-propagators in Eq. (6.4), and without loss of generality we write

$$\Phi_{1,2}(\mathbf{p}_{1,2}) = \exp\left(-\frac{1}{2}B_D p_{1,2}^2\right). \quad (6.8)$$

Then, using the vertices of Eq. (6.6), the transverse momentum distributions of the mesons at the Born level are obtained as

$$\begin{aligned} \frac{d\sigma_{\text{Born}}^{0+}}{dy dp_T^2} \Big|_{y=0} &= \frac{\exp[-\frac{1}{2}B_D p_T^2] V_0^2}{512\pi^3 B_D} \left\{ 1 - \tau \left(1 - \frac{1}{2}B_D p_T^2\right) + \frac{\tau^2}{2} \left(1 - \frac{1}{2}B_D p_T^2 + \frac{1}{8}B_D^2 p_T^4\right) \right\} \\ \frac{d\sigma_{\text{Born}}^{0-}}{dy dp_T^2} \Big|_{y=0} &= \frac{(V_1^-)^2 p_T^2}{512\pi^3 4B_D^2} \exp[-\frac{1}{2}B_D p_T^2]. \end{aligned} \quad (6.9)$$

Now, the absorptive corrections require the evaluation of the loop integral

$$\begin{aligned}
\delta\mathcal{M}(Y, 0, \mathbf{p}_1, \mathbf{p}_2) &= \int \frac{d^2\mathbf{k}}{2(2\pi)^2} T(s, \mathbf{k}) \exp\left(-\frac{1}{2}B_D(\mathbf{p}_1 + \mathbf{k})^2\right) \exp\left(-\frac{1}{2}B_D(\mathbf{p}_2 - \mathbf{k})^2\right) \\
&\times V(\mathbf{p}_1 + \mathbf{k}, \mathbf{p}_2 - \mathbf{k}) = \exp\left(-\frac{1}{2}B_D(\mathbf{p}_1^2 + \mathbf{p}_2^2)\right) \\
&\times \int \frac{d^2\mathbf{k}}{2(2\pi)^2} \exp\left(-\frac{1}{2}(B_{\text{el}}(s) + 2B_D)\mathbf{k}^2 - B_D\mathbf{k} \cdot (\mathbf{p}_1 - \mathbf{p}_2)\right) \\
&\times \sigma_{\text{tot}}^{pp}(s) V(\mathbf{p}_1 + \mathbf{k}, \mathbf{p}_2 - \mathbf{k}). \tag{6.10}
\end{aligned}$$

It is useful to introduce the dimensionless quantities

$$g_{\text{abs}} = \frac{\sigma_{\text{tot}}^{pp}(s)}{4\pi(B_{\text{el}}(s) + 2B_D)} \quad \text{and} \quad \beta = \frac{B_D}{B_{\text{el}}(s) + 2B_D}. \tag{6.11}$$

Then, the absorptive corrections are obtained as

$$\begin{aligned}
\delta\mathcal{M}^{0+}(Y, 0, \mathbf{p}_1, \mathbf{p}_2) &= g_{\text{abs}}V_0 \exp\left(-\frac{1}{2}B_D(\mathbf{p}_1^2 + \mathbf{p}_2^2)\right) \exp\left(\frac{1}{2}\beta B_D(\mathbf{p}_1 - \mathbf{p}_2)^2\right) \\
&\times \left\{1 + \beta(1 + \beta)\tau B_D(\mathbf{p}_1^2 + \mathbf{p}_2^2) + (\mathbf{p}_1 \cdot \mathbf{p}_2)\tau B_D(1 - 2\beta(1 + \beta))\right\}, \tag{6.12}
\end{aligned}$$

$$\begin{aligned}
\delta\mathcal{M}^{0-}(Y, 0, \mathbf{p}_1, \mathbf{p}_2) &= (1 - \beta)g_{\text{abs}}V_1^- \exp\left(-\frac{1}{2}B_D(\mathbf{p}_1^2 + \mathbf{p}_2^2)\right) \exp\left(\frac{1}{2}\beta B_D(\mathbf{p}_1 - \mathbf{p}_2)^2\right) \\
&\times [\mathbf{p}_1, \mathbf{p}_2](1 - \beta)(1 - \beta B_D(\mathbf{p}_1 \cdot \mathbf{p}_2)), \tag{6.13}
\end{aligned}$$

for the scalar and pseudoscalar meson, respectively. We now adjust the constants V_0, V_1^\pm , as well as B_D , to our numerical results obtained for the Born-level amplitude.

In Tables 3 and 4, we show the parameters obtained for different prescriptions for the generalized unintegrated gluon distribution, GBW as well as the CDHI and Durham prescriptions for the GJR08NLO gluon distribution. We also show the gap survival factors

$$S^2 \equiv \frac{d\sigma/dy\big|_{y=0}}{d\sigma_{\text{Born}}/dy\big|_{y=0}}. \tag{6.14}$$

We observe that depending on the gluon distribution used, we obtain for the χ_c the gap survival values of $S^2 = 0.2 \div 0.32$, while for the η_c production rather similar values $S^2 = 0.26 \div 0.3$ emerge. This similarity may be rather surprising, as the η_c amplitude, due to the vanishing in forward direction, is more peripheral than the one for χ_c production. However notice that the both reactions have significantly different values of the effective diffraction slopes B_D .

Our simplified double-Regge approach works reasonably well. In Figs. 11, 12 and 13 we show the cross section $d\sigma/dydp_T$ at $y = 0$ for the χ_c for the three different generalized UGD prescriptions. Shown is the exact numerical result of the Born amplitude (solid line) as well as the result of our effective Regge amplitude fit (long-dashed line). By the short-dashed line we show the differential cross section including absorptive corrections on top of the Regge amplitude Born term. We see from these figures that the effective Regge amplitude form is

reasonably accurate for $p_T \lesssim 1.5 \text{ GeV}$, with a slight ambiguity in the slope B_D . In the case of the η_c shown in Fig. 14, the effective Regge fit works almost perfectly for the PST-GBW and CDHI prescriptions, while for the Durham case the description is rather poor. Note however that for the η_c case the PST-GBW gives by far the largest cross section.

VII. CONCLUSION

In the present paper we have calculated the key observables of central exclusive χ_{c0} and η_c quarkonia production in proton-proton collisions at the LHC within a formalism proposed earlier ago by the Durham group for central exclusive Higgs boson production.

The χ_{c0} meson CEP was already computed in the literature previously, while η_c production has been analysed here for the first time. Compared to the previous calculations we have used modern versions of collinear gluon distributions to generate off-diagonal unintegrated gluon distributions.

In the present analysis we have also used the $gg \rightarrow \eta_c$ and $gg \rightarrow \chi_{c0}$ transition amplitudes calculated using the light-cone $c\bar{c}$ wave functions obtained in the framework of potential models. We have performed similar calculations for inclusive production of η_c and χ_{c0} very recently and showed that one can very well describe the experimental data for $\eta_c(1S)$ meson measured in last few years by the LHCb collaboration. Our previous results showed that in the inclusive case the cross section for η_c is significantly larger than that for χ_{c0} .

It was the main aim of the present paper to make a similar analysis for the exclusive production case, not done so far in the literature. In contrast to the inclusive case, we have found that for the CEP the situation reverses i.e. the corresponding cross section for exclusive η_c production is considerably smaller than its counterpart for exclusive χ_{c0} production, at least, for the hard part obtained using the Durham or Cudell et al prescriptions for calculation of the scale in the off-diagonal unintegrated gluon distribution. The reason is a specific interplay of the off-diagonal UGDs and virtual gluon – virtual gluon – quarkonium vertex.

We also proposed a way to calculate the soft effects (in the region of small gluon transverse momenta) using the GBW UGDF and a simple (PST) prescription for its off-diagonal extrapolation. In this case, the cross section is only slightly smaller for η_c than for χ_{c0} production. We have also discussed to which extent the absorption effects for $pp \rightarrow pp\eta_c$ are different than those for $pp \rightarrow pp\chi_{c0}$. We find that the absorptive corrections are rather similar in spite of very different (t_1, t_2) dependence for the corresponding Born amplitudes. However, the very different slopes of the Born-amplitudes compensate this effect to some extent.

It would be desirable to measure the cross section for $pp \rightarrow pp\eta_c$ by identifying η_c e.g. in the $p\bar{p}$ decay channel as was done in the inclusive case. It could be interesting to estimate the signal-to-background ratio before the real experiment. The $pp \rightarrow ppp\bar{p}$ continuum was calculated previously by Lebedowicz, Nachtmann and Szczurek [33] and a first experimental evidence was obtained very recently by the STAR collaboration at RHIC [34]. Also the $pp \rightarrow pp\gamma\gamma$ reaction could be considered as an alternative to measure the $pp \rightarrow pp\eta_c$ reaction.

ACKNOWLEDGMENTS

The stay of I.B. in Lund was supported by Polish National Agency for Academic Exchange under Contract No. PPN/IWA/2018/1/00031/U/0001. This study was partially supported by the Polish National Science Center under grant No. 2018/31/B/ST2/03537 and by the Center for Innovation and Transfer of Natural Sciences and Engineering Knowledge in Rzeszów (Poland). R.P. was partially supported by the Swedish Research Council grant No. 2016-05996 and by the European Research Council (ERC) under the European Union's Horizon 2020 research and innovation programme (grant agreement No 668679).

-
- [1] V. A. Khoze, A. D. Martin, M. G. Ryskin and W. J. Stirling, *Eur. Phys. J. C* **35**, 211-220 (2004);
L. A. Harland-Lang, V. A. Khoze, M. G. Ryskin and W. J. Stirling, *Int. J. Mod. Phys. A* **29**, 1430031 (2014).
 - [2] M. G. Albrow, T. D. Coughlin and J. R. Forshaw, *Prog. Part. Nucl. Phys.* **65** 149 (2010).
 - [3] R. S. Pasechnik, A. Szczurek and O. V. Teryaev, *Phys. Rev. D* **78**, 014007 (2008).
 - [4] R. S. Pasechnik, A. Szczurek and O. V. Teryaev, *Phys. Lett. B* **680**, 62 (2009).
 - [5] R. S. Pasechnik, A. Szczurek and O. V. Teryaev, *Phys. Rev. D* **81**, 034024, (2010).
 - [6] P. Lebiedowicz, O. Nachtmann and A. Szczurek, *Annals Phys.* **344**, 301-339 (2014).
 - [7] F. Kopp, M. B. Gay Ducati and M. V. T. Machado, *Phys. Lett. B* **806**, 135492 (2020).
 - [8] I. Babiarcz, R. Pasechnik, W. Schfer and A. Szczurek, *JHEP* **02**, 037 (2020).
 - [9] I. Babiarcz, R. Pasechnik, W. Schfer and A. Szczurek, *JHEP* **06**, 101 (2020).
 - [10] R. Aaij *et al.* [LHCb collaboration], *Eur. Phys. J. C* **75**, no.7, 311 (2015);
R. Aaij *et al.* [LHCb collaboration], *Eur. Phys. J. C* **80**, no.3, 191 (2020).
 - [11] Tichouk, H. Sun and X. Luo, *Phys. Rev. D* **101**, no.9, 094006 (2020).
 - [12] I. Babiarcz, V. P. Goncalves, R. Pasechnik, W. Schäfer and A. Szczurek, *Phys. Rev. D* **100**, no.5, 054018 (2019).
 - [13] A. Szczurek, R. Pasechnik and O. Teryaev, *Phys. Rev. D* **75**, 054021 (2007).
 - [14] A. Donnachie and P. V. Landshoff, *Phys. Lett. B* **185**, 403 (1987).
 - [15] A. Shuvaev, K. J. Golec-Biernat, A. D. Martin and M. Ryskin, *Phys. Rev. D* **60**, 014015 (1999).
 - [16] J. R. Cudell, A. Dechambre, O. F. Hernandez and I. P. Ivanov, *Eur. Phys. J. C* **61**, 369 (2009).
 - [17] K. J. Golec-Biernat and M. Wüsthoff, *Phys. Rev. D* **60**, 114023 (1999), K. Golec-Biernat and S. Sapeta, *JHEP* **03**, 102 (2018).
 - [18] P. Jimenez-Delgado and E. Reya, *Phys. Rev. D* **89** no.7, 074049 (2014).
 - [19] M. Gluck, P. Jimenez-Delgado, E. Reya and C. Schuck, *Phys. Lett. B* **664**, 133-138 (2008).
 - [20] M. Gluck, E. Reya and A. Vogt, *Z. Phys. C* **67**, 433-448 (1995).
 - [21] J. D. Bjorken, *Phys. Rev. D* **47**, 101-113 (1993).
 - [22] E. Gotsman, E. Levin and U. Maor, *Phys. Rev. D* **60**, 094011 (1999).
 - [23] A. B. Kaidalov, V. A. Khoze, A. D. Martin and M. G. Ryskin, *Eur. Phys. J. C* **21**, 521-529 (2001).
 - [24] S. Ostapchenko and M. Bleicher, *Eur. Phys. J. C* **78**, no.1, 67 (2018).
 - [25] C. Flensburg, G. Gustafson and L. Lönnblad, *JHEP* **1212**, 115 (2012).
 - [26] C. O. Rasmussen and T. Sjöstrand, *JHEP* **1602**, 142 (2016).

- [27] R. S. Pasechnik and B. Z. Kopeliovich, *Eur. Phys. J. C* **71**, 1827 (2011).
- [28] R. Pasechnik, B. Kopeliovich and I. Potashnikova, *Phys. Rev. D* **86**, 114039 (2012).
- [29] B. Z. Kopeliovich, R. Pasechnik and I. K. Potashnikova, *Phys. Rev. D* **98**, no. 11, 114021 (2018).
- [30] L. Lönnblad and R. lebk, *Eur. Phys. J. C* **76** (2016) no.12, 668.
- [31] I. Babiarez, R. Staszewski and A. Szczurek, *Phys. Lett. B* **771**, 532-538 (2017).
- [32] G. Antchev *et al.* [TOTEM Collaboration], *Eur. Phys. J. C* **79**, no.2, 103 (2019).
- [33] P. Lebiedowicz, O. Nachtmann and A. Szczurek, *Phys. Rev.* **D97**, 094027 (2018).
- [34] J. Adam *et al.* [STAR Collaboration], *JHEP* **07**, 178 (2020).